

# Excitation of high-amplitude localized nonlinear waves as a result of interaction of kink with attractive impurity in sine-Gordon equation

E. G. Ekomasov<sup>a</sup>, A. M. Gumerov<sup>a</sup>, R. R. Murtazin<sup>a</sup>, A. E. Ekomasov<sup>a</sup>, S. V. Dmitriev<sup>b</sup>

<sup>a</sup>*Bashkir State University, Russia, 450076, Ufa, Z. Validi Str., 32*

<sup>b</sup>*Institute for Metals Superplasticity Problems, Russian Academy of Science, Russia, 450001, Ufa, Khalturin Str. 39*

---

## Abstract

We study properties of the localized solitons to the sine-Gordon equation excited on the attractive impurity by a moving kink. The cases of one- and two-dimensional spatially extended impurities are considered. For the case of one-dimensional impurity the possibility of excitation of the first even and odd high-amplitude impurity modes by the moving kink is demonstrated. For the case of two-dimensional impurity we show the possibility of excitation of the nonlinear high-amplitude waves of new type called here breathing pulson and breathing 2D soliton. We suggest different analytical expressions to model these nonlinear excitations. The dependencies of the oscillation frequency and the amplitude of the excited impurity modes on the impurity parameters are reported.

**Keywords:** sine-Gordon equation, impurity, kink, soliton, pulson

---

## 1. Introduction

In the last years, the solitary wave dynamics has attracted increasing attention of researchers [1]. This is due to the fact that solitons initially studied in integrable systems gave rise to the study on solitary waves in non-integrable systems to describe a number of physical problems. For example, the sine-Gordon equation (SGE) is used for modeling wave propagation in geological media, in molecular biology, field theory models, in elementary particle physics, to name a few [2, 3]. The SGE soliton solutions help to describe domain walls in magnetics, dislocations in crystals, fluxons in Josephson's junctions, etc. [4–6]. In many cases behavior of solitons can be effectively described by quasi-particles and then their dynamics can be presented by ordinary differential equations [7]. However, in the presence of perturbations, the structure of solitons can be changed and they can be more accurately described by deformable quasi-particles [5]. Soliton's internal degrees of freedom can be excited in this case and they can play a very important role in a number of physical processes [8, 9]. Soliton internal modes can be responsible for the non-trivial effects of their interactions [10–14]. The internal modes can include the translational and pulsation mode describing long-lived oscillations of soliton width [15]. Effect of various perturbations on the excitation of SGE soliton's internal modes attracts a lot of attention of researchers. Local inhomogeneities are ubiquitous in many physical systems, including those described by SGE, and it is very important to study the soliton scattering on such impurities [5]. For instance, there exist many works devoted to the analysis of external force that varies in time and space [5, 9, 15–17]. Weak perturbations on the SGE solutions can be studied in frame of the perturbation theory well-developed for solitons [5, 7] but the effect of strong perturbations can be analyzed only numerically [18–20].

The effect of spatial modulation (inhomogeneity) of the periodic potential or the presence of an impurity in the system are also very interesting [5]. Depending on the geometry of the system, physically meaningful can be one-dimensional or multi-dimensional problems. The problem of scattering of SGE kinks on impurities in one-dimensional case has been under consideration for a long time [7, 19, 21, 22]. For example, the model of classical particle is applicable to the problem of kink-impurity interaction in the case when impurity itself does not support vibrational modes

---

*Email addresses:* EkomasovEG@gmail.com (E. G. Ekomasov), <http://soliton.fizfaka.net/> (E. G. Ekomasov), bgu@bk.ru (A. M. Gumerov), dmitriev.sergey.v@gmail.com (S. V. Dmitriev)

localized on the impurity [5]. Importance of the impurity modes in the mechanisms of kink-impurity interactions has been demonstrated in the works [5, 23–26]. Let us mention such an interesting effect as the reflection of kink by an attractive impurity due to the resonance energy exchange between translational kink's mode and the impurity mode.

Two-dimensional SGE has been also studied for a long time with the use of analytical methods [27–29] and with the help of numerical methods [18, 27, 30]. For example, in the works [18, 31] the appearance and motion of flexural solitary waves on the kink interacting with a two-dimensional impurity has been investigated. However, the possibility of excitation of various two-dimensional vibrational modes localized on the impurity was not discussed in those works.

In the present study we analyze the interaction of SGE kink with impurity in the case when large-amplitude nonlinear waves localized on the impurity are excited as a result of interaction.

Let us consider the system defined by the following Lagrangian

$$L(x, y, t) = \frac{1}{2} \left[ \left( \frac{\partial \theta}{\partial t} \right)^2 + \left( \frac{\partial \theta}{\partial x} \right)^2 + \left( \frac{\partial \theta}{\partial y} \right)^2 \right] \pm [1 - \Delta K(x, y)] \sin^2 \theta. \quad (1)$$

The corresponding equation of motion for the scalar field  $\theta(x, y, t)$  has the following form

$$\frac{\partial^2 \theta}{\partial t^2} - \frac{\partial^2 \theta}{\partial x^2} - \frac{\partial^2 \theta}{\partial y^2} + \frac{1}{2} K(x, y) \sin 2\theta = 0, \quad (2)$$

where the function  $K(x, y)$  defines the interaction of the field  $\theta(x, y, t)$  with the impurity.

## 2. One-dimensional case

The sine-Gordon model with the impurity extended in one dimension is defined by the Lagrangian (1) with

$$K(x) = \begin{cases} 1, & x < x_1, \ x > x_2 + W \\ 1 - \Delta K, & x_1 \leq x \leq x_2 + W \end{cases} \quad (3)$$

where  $W$  is the width of the impurity. Clearly,  $\Delta K > 0$  describes a potential well, while  $\Delta K < 0$  describes a potential barrier.

In the case  $K(x) = 1$  ( $\Delta K = 0$ ) Eq. 2 supports the exact solution in the form of topological soliton or, in other words, kink:

$$\theta(x, t) = 2 \arctan(\exp[\gamma(v_0)(x - v_0 t)]), \quad (4)$$

where  $\gamma(v_0) = (1 - v_0^2)^{-1/2}$  with a parameter  $0 < v_0 < 1$  defining the velocity of the kink. Equation (2) also admits the periodic in time solution in the form of breather,

$$\theta(x, t) = 2 \arctan \left( \frac{\sqrt{1 - \omega^2} \sin \omega t}{\omega \cosh \left[ \sqrt{1 - \omega^2} (x - x_0) \right]} \right), \quad (5)$$

where  $\omega$  is the breather frequency and  $x_0$  is the coordinate of its center.

The case of  $K(x) = 1 - \varepsilon \delta(x)$  where  $\delta(x)$  is the Dirac delta function and  $0 < \varepsilon < 1$  is a constant has been studied in [5]. It has been demonstrated that in frame of the underformable kink approximation the impurity acts as a potential and for the chosen sign of  $\varepsilon$  the potential is attractive and hence the soliton can be localized on the impurity. In the case of deformable kink, in addition to the oscillatory motion of the kink in the potential generated by the impurity, a strong modification of the kink shape, having a resonant character, can take place. The possibility of excitation of the impurity mode as a result of kink scattering that results in a considerable change of kink dynamics has also been considered. For the case of finite size impurity (in the simplest case  $K(x)$  has the form (3)) the interaction of the kink with the impurity has been analyzed for both non-deformable and deformable kinks [20, 21, 23].

Let us investigate the relation between the spectra of the impurity mode and the small-amplitude excitations of (1). We take into account that for the one-dimensional case of (2) with  $K(x) = 1$  there exists the vacuum solution  $\theta_{\pm}(x, t) = 0$ . We look for the spectrum of the small-amplitude vibrations in the vicinity of this solution

$$\theta(x, t) = \theta_{\pm} + \delta\theta(x, t), \quad \delta\theta(x, t) \ll 1. \quad (6)$$

Substituting (6) into (2) after linearization with respect to  $\delta\theta$ , one gets the equation

$$L\delta\theta(x) = \omega_n^2\delta\theta(x), \quad (7)$$

which is the Schrödinger equation with the operator  $L = -\frac{d^2}{dx^2} + K(x)$ , where  $\omega_n$  is the impurity mode frequency. Let us look for the localized solutions of the Schrödinger equation (7). It is convenient to introduce the following notations

$$\chi^2 = 1 - \omega^2, \quad k^2 = \omega^2 - (1 - \Delta K). \quad (8)$$

For  $K(x)$  defined by (3) even and odd solutions to (7) are possible [32]

$$\Psi_+ = \begin{cases} A_1^+ e^{\chi x}, & x < -W/2 \\ B_2^+ \cos kx, & -W/2 \leq x \leq W/2 \\ B_3^+ e^{\chi x}, & x > W/2 \end{cases} \quad (9)$$

$$\Psi_- = \begin{cases} A_1^- e^{\chi x}, & x < -W/2 \\ B_2^- \sin kx, & -W/2 \leq x \leq W/2 \\ B_3^- e^{\chi x}, & x > W/2 \end{cases} \quad (10)$$

We subject the solution to the condition of smoothness and continuity at the point  $x = W/2$  and obtain the following dispersion relations for even (9) and odd (10) solutions, respectively,

$$\tan\left(k\frac{W}{2}\right) = \frac{\chi}{k}, \quad (11)$$

$$\tan\left(k\frac{W}{2}\right) = -\frac{\chi}{k}. \quad (12)$$

Since, in the considered case,  $\Delta K$  and  $W$  are constant, equations (11,12) give the possibility to find all frequencies  $\omega$  of the impurity modes in the potential well of given size. The states with even and odd wave functions alternate and the first odd solution, that corresponds to the second localized state, appears when the relation  $\pi^2 = W^2\Delta K$  is satisfied.

Let us study numerically the large-amplitude localized impurity modes excited due to the interaction with a kink for the case  $\Delta K \leq 0$ . The most interesting case is when the size of the soliton is of the same order with the size of the impurity because in this case the soliton shape is strongly affected by the impurity. To solve the equations of motion (2) numerically we use the iteration method for the explicit scheme. The following algorithm was applied. Initially we have a SGE kink (4) moving with a constant speed. Boundary conditions have the form  $\theta(\pm\infty) = 0, \pi$ ;  $\theta'(\pm\infty) = 0$ . We introduce the mesh for the spatial coordinate and iterate with respect to time, taking into account the convergence condition for the explicit scheme, to find the kink position at the next time step. The characteristics of the nonlinear wave were found from the numerically constructed function  $\theta(x, t)$ .

The numerical experiments have demonstrated that the kink passing the impurity excites the bell-shaped nonlinear oscillatory wave, see Fig. 1. We found that this oscillatory mode can be well fitted by the expression

$$\theta^*(x, t) = A \exp(-\alpha(t - t_0)) \arctan\left(\frac{\sqrt{1 - \omega^2} \sin[\omega\gamma(t - t_0)]}{\omega \operatorname{sech}(\gamma \sqrt{1 - \omega^2} x)}\right), \quad (13)$$

which is a stationary breather (5) in the presence of damping with the coefficient  $\alpha$  and with an additional fitting parameter  $\gamma$ . In Fig. 2 we compare the numerically found time evolution of the field value at the center of the impurity ( $x = 0$ ) with that found from the approximating formula (13) with the fitting parameters  $A = 0.4$ ,  $\omega = 0.616$ ,  $\alpha = 4.5 \times 10^{-5}$ ,  $\gamma = 1$ ,  $t_0 = 4.5$ . The numerical result and the result obtained from the fitting formula (13) overlap. Damping of the breather is due to slow radiation of small-amplitude extended waves that can be seen in Fig. 1.

Amplitude of the breather excited by the passing kink depends on the kink velocity  $v_0$  (see Fig. 3) and the curve has a maximum with the value dependent on the impurity parameters  $\Delta K$  and  $W$ .

The amplitude of the excited breather also depends on  $\Delta K$  and  $W$  and it vanishes when  $\Delta K \rightarrow 0$ ,  $W \rightarrow 0$ , i.e., in the absence of impurity.

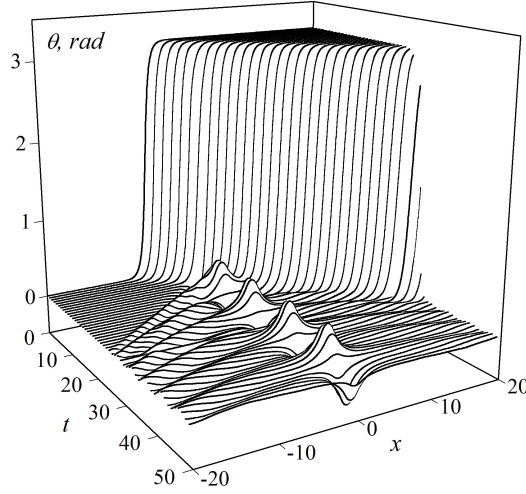


Figure 1: Excitation of the breathing nonlinear excitation on the impurity by the moving kink for the case of  $\Delta K = 1.5$ ,  $W = 1.5$ ,  $v_0 = 0.86$ . The impurity center is located at  $x = 0$ .

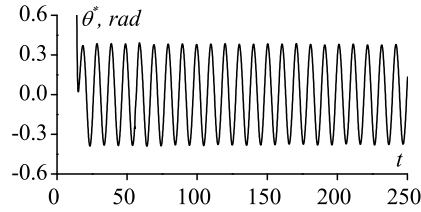


Figure 2: Time dependence of the field value at the center of the impurity showing the oscillation of the breather excited by the passing kink as shown in Fig.1. The numerically obtained result overlaps with that calculated from (13) for  $x = 0$  and  $A = 0.4$ ,  $\omega = 0.616$ ,  $\alpha = 4.5 \times 10^{-5}$ ,  $\gamma = 1$ ,  $t_0 = 4.5$ .

Breather frequency  $\omega_B$  is practically independent of the kink velocity  $v_0$ , while it depends on  $\Delta K$  and  $W$  as shown in Fig. 4.

It can be seen that for  $\Delta K \rightarrow 0$ ,  $W \rightarrow 0$  the breather frequency tends to unity but the frequencies of kink's translational and pulsation (oscillation of kink width) modes excited due to the interaction with impurity tend to zero [20]. This behavior can be easily understood taking into account that breather energy scales as  $E \sim (1 - \omega_B^2)^{1/2}$  [2] meaning that for vanishing size of the impurity the energy and the amplitude of the breather also vanish. It can also be seen that the linear approximation for the first even solution described above gives a good description of the excited breathers in the range of small amplitudes because the frequencies calculated from the analytical expression (11) (solid lines in Fig. 4) coincide with the frequencies found numerically by solving (2). Excitation of the first odd mode (the second main state) will be discussed for the case of kink pinning by the impurity. In this case, as it was already mentioned, pulsation and translational modes can be excited on the kink [20]. In the case when kink pulsation mode frequency  $\omega_{pulse} < 1$ , after a transient period a state is formed that can be described with a good accuracy by the kink-type solution. Therefore, in our case the most interesting is the range of parameters  $\Delta K$  and  $W$  where  $\omega_{pulse} \rightarrow 1$  and the excited nonlinear wave (see Fig. 5a) differs considerably from the kink solution (see Fig. 5b). Algebraic difference of the solutions has the form dramatically different from that shown in Fig. 1 and it is analogous to the form of the odd solutions to the Schrödinger equation.

One should also take into account that for the case of large-amplitude nonlinear waves obtained numerically, a three-kink solution can be not just a linear sum of the kink and breather solutions but a modified solution that takes into account kink vibrations described by the wobble SGE solution [33, 34]. For yet increasing values of  $\Delta K$  and  $W$

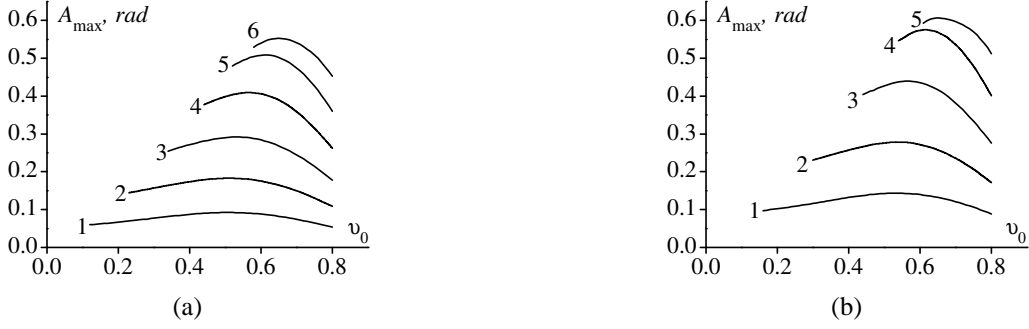


Figure 3: Breather amplitude  $A_{\max}$  measured at the impurity center as the function of kink velocity  $v_0$  for (a)  $W = 1$  and (b)  $W = 1.5$ . Curves 1 to 6 are for  $\Delta K = \{0.5, 0.75, 1, 1.25, 1.5, 1.75\}$ , respectively.

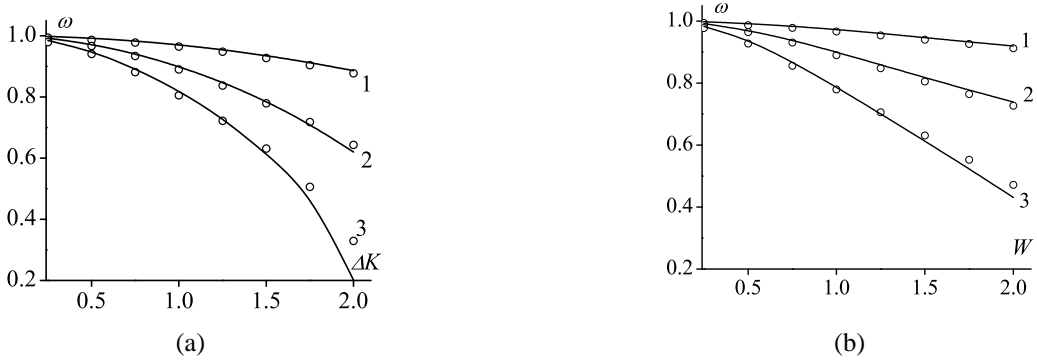


Figure 4: Dependence of the breather oscillation frequency on the parameters  $\Delta K$  (a) and  $W$  (b). The solid line corresponds to the frequency calculated from (11), while scattered data was obtained by numerical integration of (2). In (a) curves 1 to 3 correspond to  $W = 0.5$ ,  $W = 1$ , and  $W = 1.5$ , respectively, while in (b) to  $\Delta K = 0.5$ ,  $\Delta K = 1$ , and  $\Delta K = 1.5$ , respectively.

let us take into account that, as it has been shown in [4], at the critical value of parameters,

$$KW = 2, \quad (14)$$

in the vicinity of the impurity a stable static soliton can exist whose amplitude can be estimated as

$$\cos A_{\max} = 2/KW, \quad (15)$$

where  $K = 1 - \Delta K$ . Numerical results show that for sufficiently large  $\Delta K$  and  $W$  after the passing of kink, in the vicinity of the impurity a soliton is formed. The dependence of soliton amplitude on  $\Delta K$  and  $W$  (see Fig. 6) can be approximately expressed as  $\cos A = 1.8/KW$ . In Fig. 7 the ranges of the impurity parameters where the breather and the soliton can exist are presented and for comparison the curve defined by (14) is plotted.

### 3. Two-dimensional case

For definiteness let us take the impurity in the following form [18]

$$K(x, y) = \begin{cases} 1, & x < x_1, x > x_2, y < y_1, y > y_2 \\ 1 - \Delta K, & x_1 \leq x \leq x_2, y_1 \leq y \leq y_2 \end{cases} \quad (16)$$

where  $W_x = x_1 - x_2$  and  $W_y = y_1 - y_2$  are the parameters that specify the size of the impurity. Similarly to the one-dimensional case, Eq. (2) was integrated with the use of an explicit scheme. A uniform mesh with the step  $\xi$  was introduced for  $x$  and  $y$  coordinates,

$$x_i = \xi i, \quad i = -N_x, \dots, N_x, \quad y_j = \xi j, \quad j = -N_y, \dots, N_y, \quad (17)$$

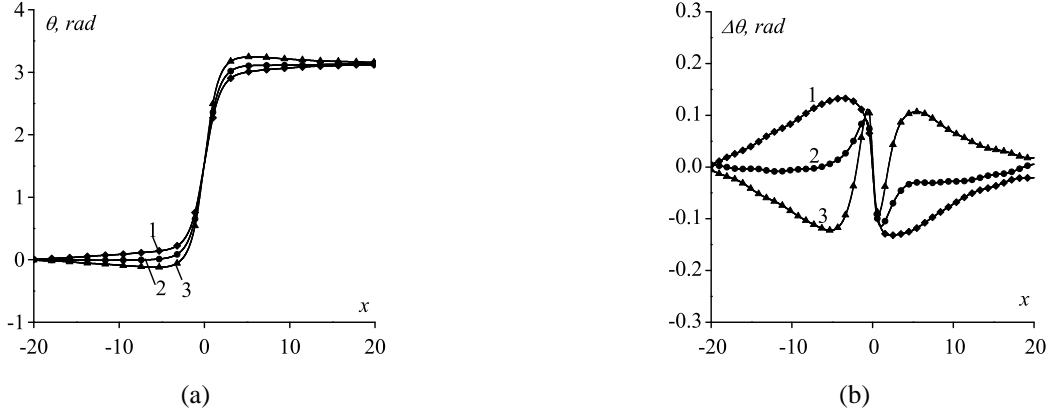


Figure 5: (a) Wobble kink profile and (b) its difference from the kink solution at different times, 1 –  $t = 1179.37$ , 2 –  $t = 1180.87$ , and 3 –  $t = 1182.37$ , for the case  $W = 1$ ,  $\Delta K = 1.2$  and initial kink velocity  $v_0 = 0.2$ . The impurity center is at  $x^* = -0.5$ .

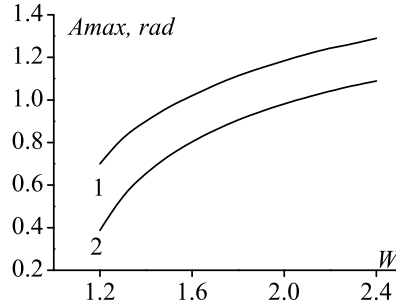


Figure 6: The dependence of the stabilized soliton amplitude on the impurity width  $W$  at fixed  $\Delta K = 2.8$ . Curve 1 gives numerical result, while curve 2 corresponds to (15).

and for the time  $t$  the mesh with the time step  $\tau$  was employed,

$$t_n = \tau n, \quad n = 0, 1, \dots, N_t, \quad (18)$$

where  $N_x$ ,  $N_y$ ,  $N_t$  are integers. For  $N_x$  and  $N_y$  we took the values from 512 to 2048. It was confirmed that the number of mesh points for the spatial coordinates does not affect the main numerical results. Initially we have a SGE kink (4) moving with constant velocity. The boundary conditions for the  $x$ -coordinate have the form  $\theta(\pm N_x \xi, y) = \theta_0(\pm N_x \xi)$ ;  $\theta'(\pm N_x \xi, y) = \theta'_0(\pm N_x \xi)$  and for the  $y$ -coordinate free edges are simulated.

Let us consider the case of  $\Delta K > 0$  when, as it was shown above, nonlinear waves localized at the impurity are excited due to the interaction with the kink. In Fig. 8 the process of kink-impurity interaction is presented and one can see that the nonlinear localized wave radiating extended waves is excited. The wave is called here breathing pulson. If  $W_x = W_y$  then the breathing pulson is symmetric with respect to  $x$  and  $y$  axis (Fig. 9a,b) and the symmetry is lost for  $W_x \neq W_y$  (Fig. 9c,d). Firstly, the excited localized wave has a bell shape and later ( $t > 20$ , curve 1 in Fig. 10) the periodic oscillations can be seen at the center of the impurity having coordinates  $(x^*, y^*)$ . With increase in the impurity size the oscillation frequency reduces. The amplitude decreases with time owing to the radiation of extended waves. It should be noted that the extended waves cannot be described by the harmonic function because they have a nonlinear nature (see Fig. 11). The breathing pulson can be regarded as a long-lived nonlinear excitation.

It is well-known that SGE supports the 2D solution called pulson describing long-lived spatially localized vibra-

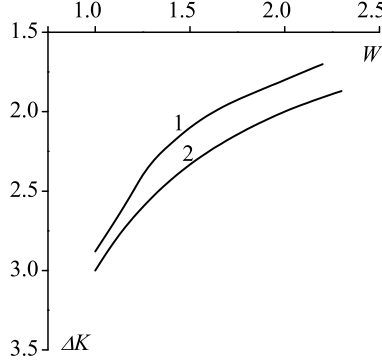


Figure 7: Space of impurity parameters showing the range where passing kink excites a breather (above the lines 1 and 2), or a soliton (below the lines 1 and 2). Line 1 was found numerically and line 2 is given by (14).

tions [27–29]. The numerically found breathing pulson can be well approximated by the expression

$$\theta(r, t) = A \arctan \left[ \frac{\sqrt{1 - \omega_p^2}}{\omega_p} \operatorname{sech} \left( \sqrt{1 - \omega_p^2} B r \right) \sin[\omega_p(t - t_0)] \right], \quad (19)$$

where  $r = \sqrt{(x/\Delta_x)^2 + (y/\Delta_y)^2}$ , with  $\Delta_x$  and  $\Delta_y$  being the pulson width along  $x$  and  $y$  axis, respectively. For example, for the curve 1 in Fig. 10 one should set in (19)  $r = 0$  and  $A = 0.42$ ,  $\omega_p = 0.85$ ,  $B = 4.8$ ,  $t_0 = 2.5$ ,  $\Delta_x = 2.4$ , and  $\Delta_y = 3.4$ .

Our numerical results show that the breathing pulson frequency  $\omega_p$  [determined from  $\theta(x^*, y^*, t)$ ] does not depend on kink velocity  $v_0$ , but it is a function of  $W_x$ ,  $W_y$  and  $\Delta K$ . In Fig. 12 the dependence of  $\omega_p$  on the parameters  $\Delta K$  and  $W_y$  is shown. It can be seen that with decrease in the impurity size the breathing pulson frequency (similar to what was observed for the breather) tends to unity. Dependence of  $\omega_p$  on  $K = 1 - \Delta K$  can be approximately given by  $\omega_p = (a(|K^*| + K))^q / \sqrt{1 + (a(|K^*| + K))^{2q}}$ , where  $a$  is a constant,  $q \approx 2$ ,  $K^*$  is the smallest value of  $K$  when breathing pulson is still formed in the vicinity of the impurity. Dependence of  $\omega_p$  on  $W_y$  (as well as on  $W_x$ ) can be approximately expressed as  $\omega_p = 1 - (bW_y)^p / \sqrt{1 + (bW_y)^{2p}}$ , where  $b$  is a constant and  $p \approx 2$ . Maximal breathing pulson amplitude,  $A_{\max}$ , as the function of the kink velocity  $v_0$  is presented in Fig. 13 and, similarly to the one-dimensional case, it has a maximum. With decrease in the impurity size  $A_{\max}$  vanishes. The dependence  $A_{\max}(\Delta K)$  for small values of  $\Delta K$  is close to linear. The dependence  $A_{\max}(W_y)$  for  $W_y < 1$  is close to linear and for large  $W_y$  it saturates. Note that for fixed  $v_0$  maximal value of  $A_{\max}$  strongly depends on  $\Delta K$ ,  $W_x$  and  $W_y$ .

For increasing values of the parameters  $\Delta K$ ,  $W_x$  and  $W_y$ , after the kink passes the impurity, a localized nonlinear wave called here breathing 2D soliton is excited on the impurity (see Fig. 14). The breathing 2D soliton shape depends on the parameters  $W_x$  and  $W_y$  and it can be symmetric (Fig. 15a,b) or asymmetric (Fig. 15c,d). Our numerical results suggest that the breathing 2D soliton is a long-lived excitation with amplitude slowly decreasing in time. The breathing 2D soliton cannot be described by the direct sum of 2D soliton solution and pulson solution to SGE. On the other hand, the breathing 2D soliton can be well approximated by the expression

$$\theta(r, t) = \arctan \left( \frac{A_0 + A_1 \sin[\omega_S(t - t_0)]}{\omega_S^{-1} \sqrt{1 - \omega_S^2} \cosh(\sqrt{1 - \omega_S^2} B r)} \right), \quad (20)$$

where  $r = \sqrt{(x/\Delta_x)^2 + (y/\Delta_y)^2}$ ,  $B = B_0 - B_1 \sin[\omega_S(t - t_0)]$ ,  $\omega_S$  is breathing 2D soliton frequency,  $A_0$ ,  $A_1$ ,  $B_0$ ,  $B_1$  are the breathing 2D soliton parameters that depend on the impurity parameters,  $\Delta_x$ ,  $\Delta_y$  are the characteristic widths of the soliton along  $X$  and  $Y$  axis, respectively. For example, the curve 2 in Fig. 10 is well fitted by (20) with  $r = 0$  and  $A_0 = 0.63$ ,  $A_1 = 0.13$ ,  $B_0 = 9$ ,  $B_1 = 1$ ,  $\omega_S = 0.94$ ,  $t_0 = 0$ ,  $\Delta_x = 1.8$ , and  $\Delta_y = 3.2$ .

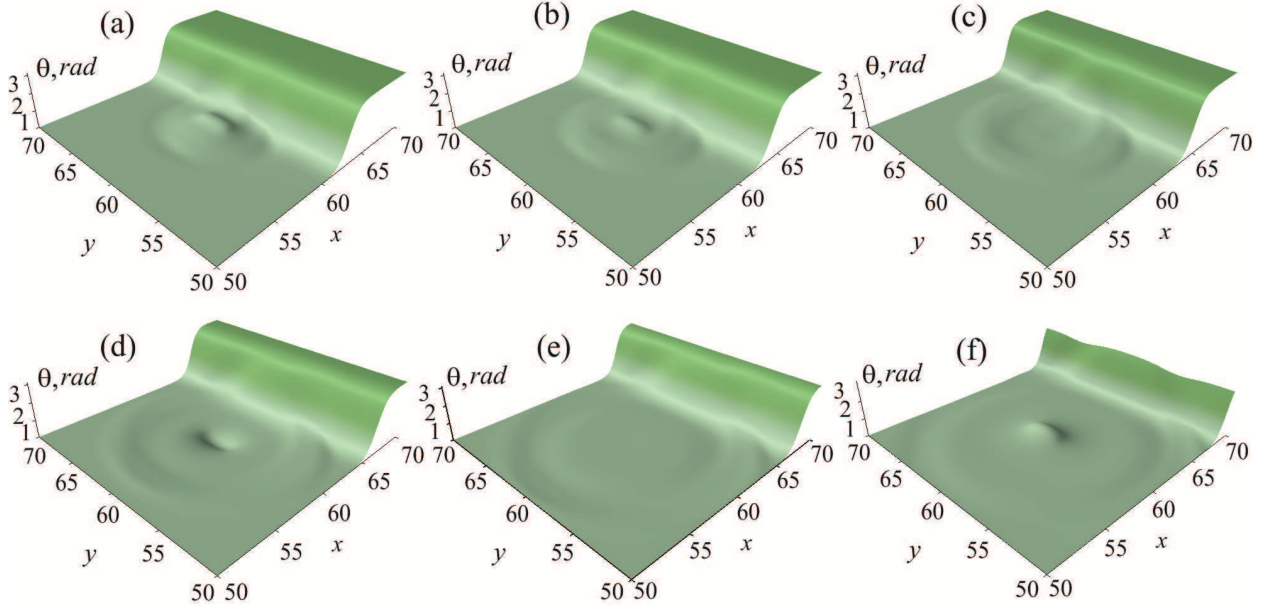


Figure 8: The excitation and evolution of a breathing pulson for the case  $W_x = 1$ ,  $W_y = 3$ , and  $\Delta K = 2$ . (a)  $t = 11.55$ , (b)  $t = 12.6$ , (c)  $t = 13.65$ , (d)  $t = 15.75$ , (e)  $t = 17.43$ , and (f)  $t = 19.32$ . The impurity center coordinates are  $x^* = y^* = 60$ .

Our numerical results have demonstrated that the breathing 2D soliton frequency,  $\omega_S$ , similarly to what was observed for the pulson, does not depend on the initial kink velocity but is a function of the parameters  $W_x$ ,  $W_y$  and  $\Delta K$  (see Fig. 16). It can be seen that  $\omega_S$  tends to unity for increasing  $W_x$ ,  $W_y$  and  $\Delta K$ . The dependence of  $\omega_S$  on  $K = 1 - \Delta K$  can be approximated by the expression  $\omega_S = (c(|K^*| - K))^q / \sqrt{1 + (c(|K^*| - K))^{2q}}$ , where  $q \approx 6$ ,  $c$  is a constant, and  $K^*$  is the largest value of  $K$  at which the breathing 2D soliton can be formed in the impurity region. The dependence of  $\omega_S$  on  $W_y$  (as well as on  $W_x$ ) can be approximately given by  $\omega_S = (aW_y)^p / \sqrt{1 + (aW_y)^{2p}}$ , where  $p \approx 3$ , and  $a$  is a constant. In Fig. 17 for the breathing 2D soliton we present the dependence of  $\Delta_y$  on the parameters  $W_y$ . It can be seen that  $\Delta_y$  depends almost linearly on  $W_y$ . The relation between parameters describing the size of impurity and the width of the breathing 2D soliton can be approximately written as

$$\frac{\Delta_x^2}{W_x^2} + \frac{\Delta_y^2}{W_y^2} = R^2, \quad (21)$$

where for the symmetric impurity region  $R = 2^{3/4}$ , and, in general, parameter  $R$  depends on the parameters  $\Delta K$ ,  $W_x$  and  $W_y$ .

In Fig. 18 we plot the regions of the parameters  $\Delta K$ ,  $W_x$  and  $W_y$  where different localized nonlinear excitations exist. It can be seen that the increase in  $W_y$  shifts the critical curves toward the smaller values of the parameters  $\Delta K$  and  $W_x$ .

#### 4. Conclusions

Using analytical and numerical methods we examined the dynamics of the sine-Gordon equation kinks passing through the attractive impurity. The cases of extended one-dimensional and two-dimensional impurities were studied.

By linearizing the sine-Gordon equation we obtained the dispersion relations for the small-amplitude localized impurity modes. Using numerical methods we showed the possibility of excitation by the passing kink of the first even and odd modes of high-amplitude localized on the impurity modes. The obtained numerically dispersion relations in the case of low oscillation amplitudes are in good agreement with the results of analytical calculations.

For the case of two-dimensional impurity we showed numerically the possibility of excitation by the passing kink of non-linear high-amplitude waves of new type, called here breathing pulson and breathing 2D soliton. We



suggested analytical expressions to model these new excitations. The breathing pulson and breathing 2D soliton radiate extended waves and their amplitudes slowly decrease. Both excitations are long-living and can be of both symmetric and asymmetric type depending on the impurity type. We determined the range of the impurity parameters where the breathing pulson and breathing 2D soliton can be excited. The amplitude, size and frequency of the excited localized nonlinear as the functions of the impurity parameters were given.

## Acknowledgements

The work was partly supported by the Russian Foundation for Basic Research, grants 11-08-97057-p-povolzhie-a and 10-02-00594-a.

## References

- [1] P. L. Christiansen, M. P. Sorensen, A. C. Scott (Eds.), *Nonlinear science at the dawn of the 21st century*, Springer, Berlin, 2000.
- [2] A. C. Scott (Ed.), *Encyclopedia of Nonlinear Science*, Routledge, New York, 2004.
- [3] L. V. Yakushevich, A. V. Savin, L. I. Manevitch, On the internal dynamics of topological solitons in dna, *Phys. Rev. E* 66 (2002) 016614–016629.
- [4] E. G. Ekomasov, S. A. Azamatov, R. R. Murtazin, Studying the nucleation and evolution of magnetic inhomogeneities of the soliton and breather type in magnetic materials with local inhomogeneities of anisotropy, *The Physics of Metals and Metallography* 105 (2008) 313–321.
- [5] O. M. Braun, Y. S. Kivshar, *The Frenkel-Kontorova Model: Concepts, Methods, and Applications*, Springer-Verlag, Berlin, 2004.
- [6] D. R. Gulevich, F. V. Kusmartsev, Perturbation theory for localized solutions of the sine-gordon equation: Decay of a breather and pinning by a microresistor, *Phys. Rev. B* 74 (2006) 214303.
- [7] M. B. Fogel, S. E. Trullinger, A. R. Bishop, J. A. Krumhandl, Dynamics of sine-gordon solitons in the presence of perturbations, *Phys. Rev. B* 15 (1977) 1578–1592.
- [8] Y. S. Kivshar, D. E. Pelinovsky, T. Cretegny, M. Peyrard, Internal modes of solitary waves, *Phys. Rev. Lett.* 80 (1998) 5032–5035.
- [9] Y. S. Kivshar, B. A. Malomed, F. Zhang, L. Vazquez, Creation of sine-gordon solitons by a pulse force, *Phys. Rev. B* 43 (1991) 1098–1109.
- [10] S. Dmitriev, A. Wusatowska-Sarnek, L. Nauman, M. Starostenkov, Generation and annihilation of dislocations in the discrete frenkel-kontorova model, *Physica Status Solidi (B)* 201 (1997) 89–96.
- [11] S. Dmitriev, L. Nauman, A. Ovcharov, M. Starostenkov, Dislocation nucleation mechanism in a one-dimensional model of a frenkel-kontorova crystal, *Russian Physics Journal* 39 (1996) 164–167.
- [12] S. Dmitriev, P. Kevrekidis, Y. Kivshar, Radiationless energy exchange in three-soliton collisions, *Phys. Rev. E* 78 (2008) 046604.
- [13] S. Dmitriev, Y. Kivshar, T. Shigenari, Fractal structures and multiparticle effects in soliton scattering, *Phys. Rev. E* 64 (2001) 056613.
- [14] S. Dmitriev, D. Semagin, T. Shigenari, A. Sukhorukov, Chaotic character of two-soliton collisions in the weakly perturbed nonlinear schrodinger equation, *Phys. Rev. E* 66 (2002) 046609.
- [15] J. A. González, A. Bellorín, L. E. Guerrero, Internal modes of sine-gordon solitons in the presence of spatiotemporal perturbations, *Phys. Rev. E* 65 (2002) 065601.
- [16] R. Chacón, A. Bellorín, L. E. Guerrero, J. A. González, Spatiotemporal chaos in sine-gordon systems subjected to wave fields: Onset and suppression, *Phys. Rev. E* 77 (2008) 046212.
- [17] C. R. Willis, Comment on existence of internal modes of sine-gordon kinks, *Phys. Rev. E* 73 (2006) 068601.
- [18] A. G. Bratsos, The solution of the two-dimensional sine-gordon equation using the method of lines, *Journal of Computational and Applied Mathematics* 206 (2007) 251–277.
- [19] J. P. Currie, S. E. Trullinger, A. R. Bishop, J. A. Krumhandl, Numerical simulation of sine-gordon soliton dynamics in the presence of perturbations, *Phys. Rev. B* 15 (1977) 5567–5580.
- [20] E. G. Ekomasov, M. A. Shabalin, Simulation the nonlinear dynamics of domain walls in weak ferromagnets, *The Physics of Metals and Metallography* 101 (2006) S48–S50.
- [21] D. I. Paul, Soliton theory and the dynamics of a ferromagnetic domain wall, *J. Phys. C: Solid State Phys* 12 (1979) 585–593.
- [22] F. Zhang, Y. S. Kivshar, L. Vazquez, Resonant kink-impurity interactions in the sine-gordon model, *Phys. Rev. A* 45 (1992) 6019–6030.
- [23] B. Piette, W. J. Zakrzewski, Scattering of sine-gordon kinks on potential wells, *J. Phys. A: Math. Gen.* 40 (2007) 5995–6010.
- [24] B. Piette, W. J. Zakrzewski, J. Brand, Scattering of topological solitons on holes and barriers, *J. Phys. A: Math. Gen.* 38 (2005) 10403–10412.
- [25] B. Piette, W. J. Zakrzewski, Dynamical properties of a soliton in a potential well, *J. Phys. A: Math. Gen.* 40 (2007) 320–346.
- [26] K. Javidan, Analytical formulation for soliton-potential dynamics, *Phys. Rev. E* 78 (2008) 046607.
- [27] R. K. Dodd, J. C. Eilbeck, J. D. Gibbon, H. C. Morris, *Solitons and nonlinear wave equations*, Academic Press, London, 1982.
- [28] M. Qing, H. Bin, R. Weigu, L. Yao, New exact solutions of the (n+1)-dimensional sine-gordon equation using double elliptic equation method, *International Journal of Computer Mathematics* 87 (2010) 591–606.
- [29] V. A. Koutvitsky, E. M. Maslov, Parametric instability of the real scalar pulsions, *Phys. Lett. A* 336 (2005) 31–36.
- [30] M. Dehghan, A. Shokri, A numerical method for solution of the two-dimensional sine-gordon equation using the radial basis functions, *Mathematics and Computers in Simulation* 79 (2008) 700–715.
- [31] E. G. Ekomasov, S. A. Azamatov, R. R. Murtazin, Excitation of nonlinear solitary flexural waves in a moving domain wall, *The Physics of Metals and Metallography* 108 (2009) 532–537.
- [32] L. D. Landau, E. M. Lifshitz, *Quantum Mechanics: Non-Relativistic Theory*, volume 3, Butterworth-Heinemann, 1977.
- [33] L. A. Ferreira, B. Piette, W. J. Zakrzewski, Wobbles and other kink-breather solutions of sine-gordon model, *Phys. Rev. E* 77 (2008) 036616.
- [34] G. Kälberman, The sine-gordon wobble, *J. Phys. A: Math. Gen.* 37 (2004) 11603–11612.

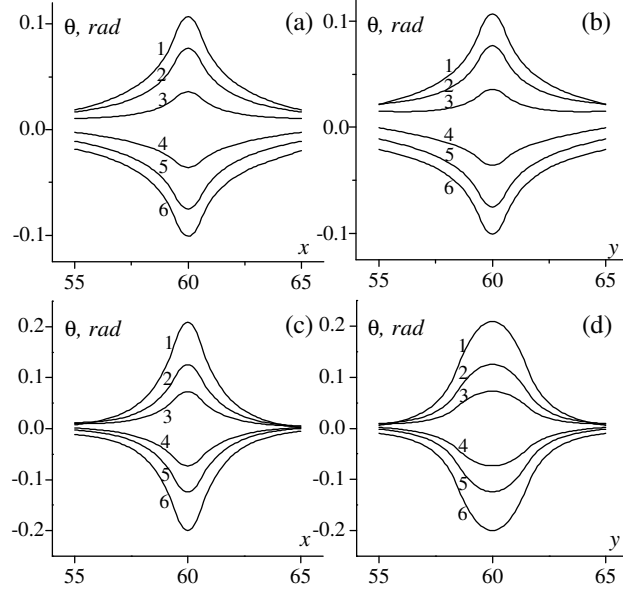


Figure 9: Snapshots of the functions  $\theta(x, y^*, t)$  (a,c) and  $\theta(x^*, y, t)$  (b,d) for the case  $\Delta K = 2$ ,  $v_0 = 0.57$ . In (a,b) the impurity is symmetric,  $W_x = W_y = 1$ , and the curves 1 to 6 are for  $t = \{28.2, 29.04, 29.5, 30.24, 30.72, 31.5\}$ . In (c,d) the impurity is asymmetric,  $W_x = 1$ ,  $W_y = 3$ , and the curves 1 to 6 are for  $t = \{44.28, 45.6, 45.96, 46.5, 46.86, 48.18\}$ . The impurity center coordinates are  $x^* = y^* = 60$ .

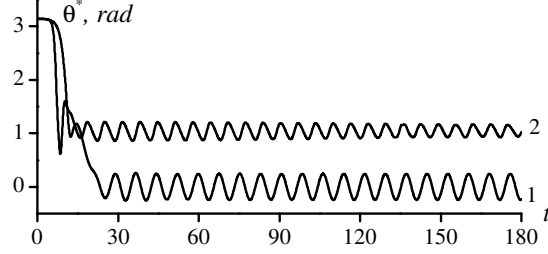


Figure 10: The function  $\theta(x^*, y^*, t)$  for the case  $v_0 = 0.85$ ,  $W_x = 1$ ,  $W_y = 3$ ,  $\Delta K = 2$  (curve 1) and  $\Delta K = 5$  (curve 2).

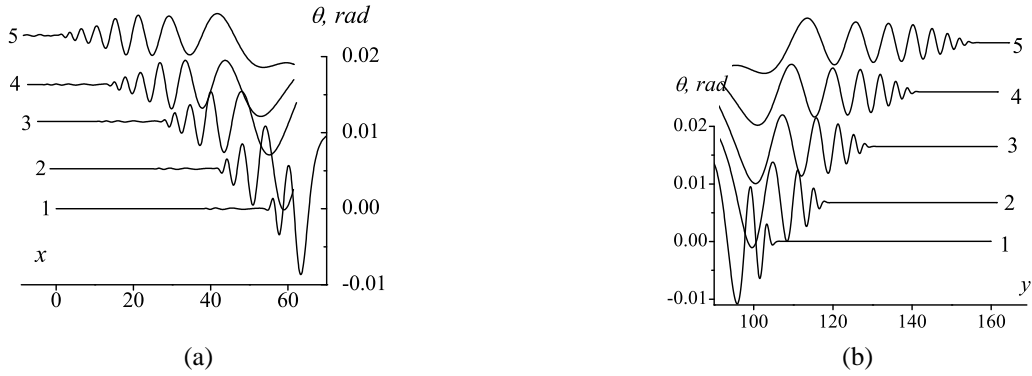


Figure 11: Snapshots of  $\theta(x, y^*, t)$  (a) and  $\theta(x^*, y, t)$  (b) for  $W_x = 1$ ,  $W_y = 1$ ,  $\Delta K = 2$ . Curves 1 to 5 correspond to  $t = \{42, 54, 66, 78, 90\}$ .

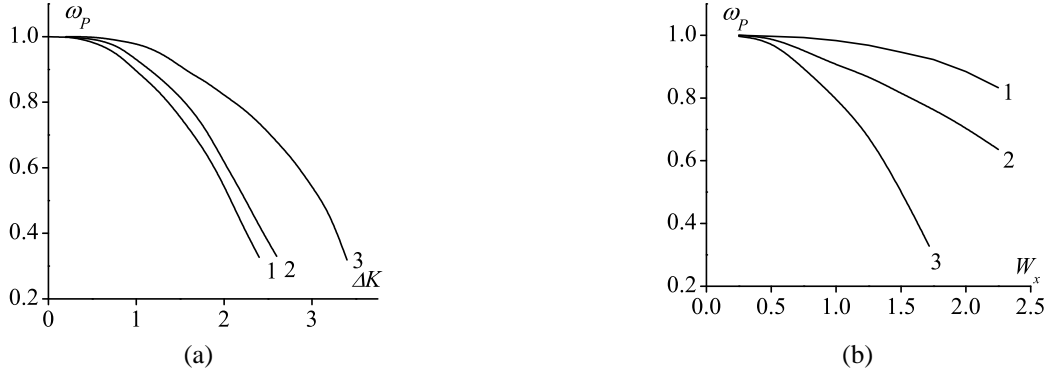


Figure 12: The dependence of the breathing pulson oscillation frequency  $\omega_p$  (a) on the parameter  $\Delta K$  for the case  $W_y = 3$  and  $W_x = 1$  (curve 1),  $W_x = 2$  (curve 2), and  $W_x = 3$  (curve 3); (b) on the parameter  $W_x$  for the case  $W_y = 1$  and  $\Delta K = 2$  (curve 1),  $\Delta K = 3$  (curve 2), and  $\Delta K = 4$  (curve 3). Kink initial velocity is  $v_0 = 0.57$ .

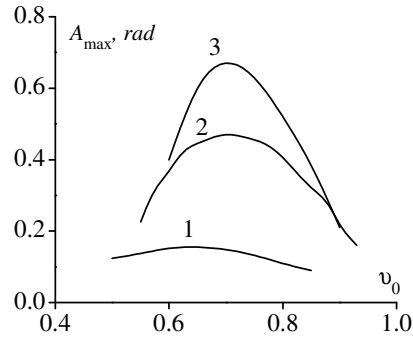


Figure 13: The dependence of the breathing pulson maximum amplitude  $A_{\max}$  at the impurity center on the kink velocity  $v_0$  for the case  $W_x = 1$ ,  $\Delta K = 2$ , and  $W_y = 1$  (curve 1),  $W_y = 2$  (curve 2),  $W_y = 3$  (curve 3).

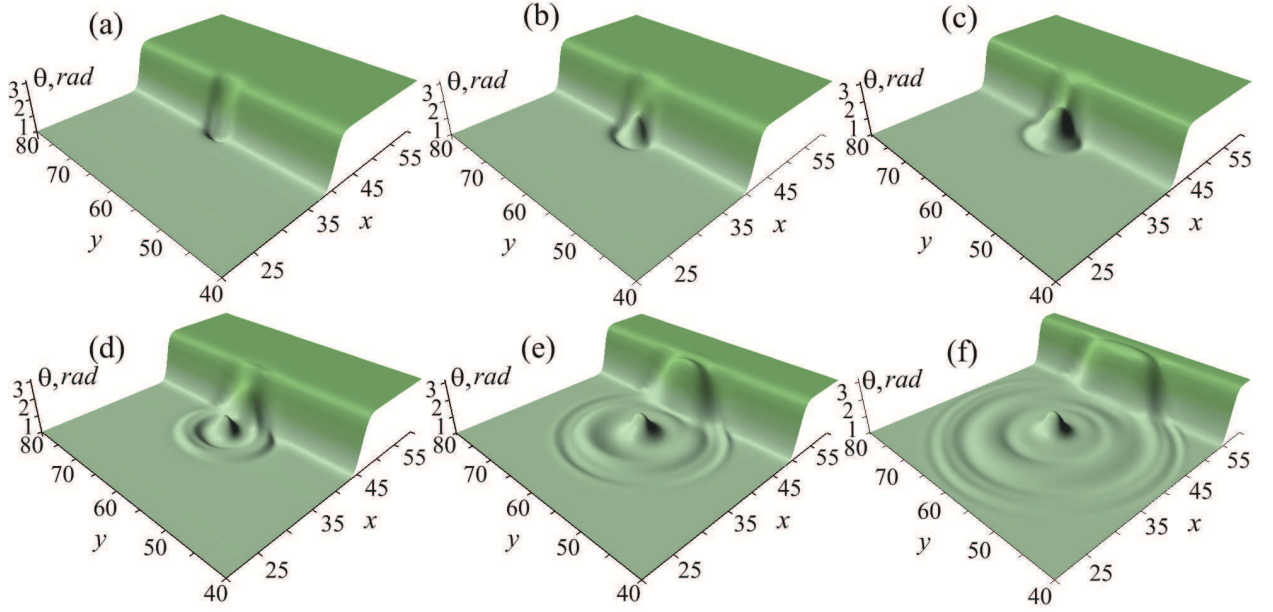


Figure 14: Excitation and evolution of the breathing 2D soliton for the case  $W_x = 1$ ,  $W_y = 3$ ,  $\Delta K = 5$ . Panels (a) to (f) correspond to  $t = \{8, 9.4, 11, 14, 20, 26\}$ . The impurity center coordinates are  $x^* = y^* = 60$ .

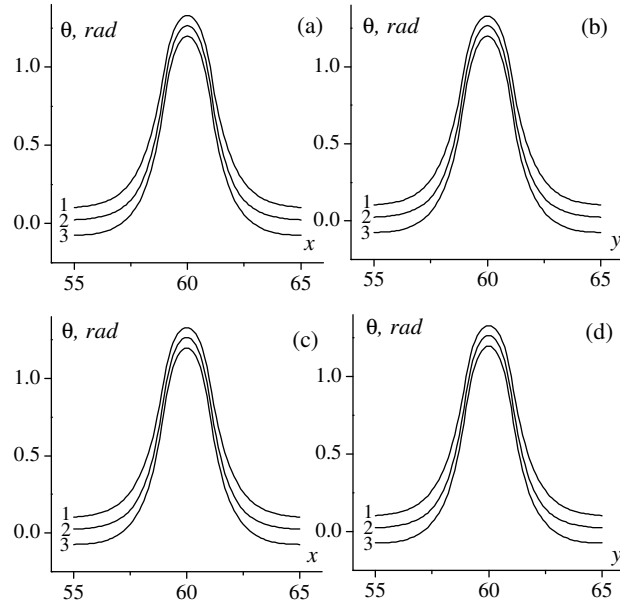


Figure 15: Snapshots of the functions  $\theta(x, y^*, t)$  (a,c) and  $\theta(x^*, y, t)$  (b,d) for the case (a,b)  $W_x = 2$ ,  $W_y = 2$ , and  $t = 30.18$  (curve 1),  $t = 31.8$  (curve 2),  $t = 33.72$  (curve 3); (c,d)  $W_x = 2$ ,  $W_y = 3$ , and  $t = 30.78$  (curve 1),  $t = 32.4$  (curve 2),  $t = 34.02$  (curve 3).  $\Delta K = 5$ ,  $v_0 = 0.85$ . The impurity center coordinates are  $x^* = y^* = 60$ .

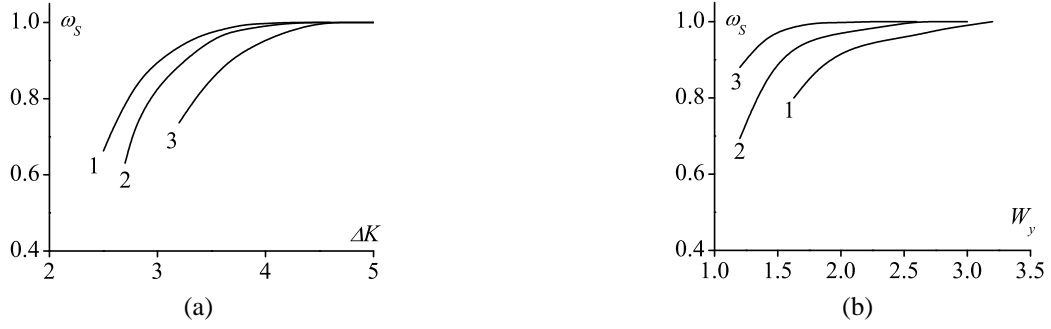


Figure 16: The dependence of the breathing 2D soliton oscillation frequency  $\omega_s$  (a) on the parameter  $\Delta K$  for the case  $W_y = 2$  and  $W_x = 2$  (curve 1),  $W_x = 3$  (curve 2),  $W_x = 4$  (curve 3); and (b) on the parameter  $W_y$  for the case  $W_x = 1$  and  $\Delta K = 5$  (curve 1),  $\Delta K = 5.5$  (curve 2),  $\Delta K = 6$  (curve 3). Initial kink velocity is  $v_0 = 0.85$ .

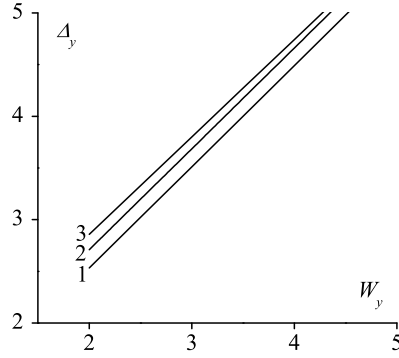


Figure 17: The breathing 2D soliton width  $\Delta_y$  as the function of the parameter  $W_y$  for  $\Delta K = 5$ ,  $v_0 = 0.85$ , and  $W_x = 2$  (curve 1),  $W_x = 3$  (curve 2),  $W_x = 4$  (curve 3).

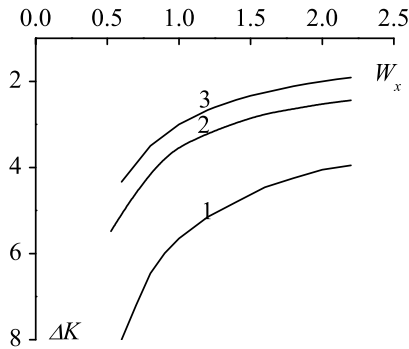


Figure 18: The regions of the impurity parameters allowing the existence of the breathing pulson (above the lines 1, 2 and 3), and the breathing 2D soliton (below the lines 1, 2 and 3). The lines 1 and 2 and 3 present numerical results for  $W_y = 1$  and  $W_y = 3$ , respectively, while line 3 is plotted with the help of (14).